Research Paper
Computational Methods for Differential Equations
http://cmde.tabrizu.ac.ir
Vol. *, No. *, *, pp. 1-18
DOI:10.22034/cmde.2026.70649.3536

Nature inspired based Metaheuristic optimization algorithm with applications to fractional Black–Scholes European option pricing model

Uroosa Arshad[1] **and Mariam Sultana**[2,*]

[1]Department of Mathematical Sciences, Federal Urdu University of Arts, Sciences & Technology, Karachi-75300, Pakistan.

[2]Institute of Space Science and Technology, University of Karachi, Karachi, Pakistan.

Abstract

This work examines the numerical approximation of the Fractional Black–Scholes European option pricing model. The text presents the creation of the Fractional Novel Analytic Genetic Algorithm (FNAGA). This newly introduced method is used to enhance an error-based fitness function that originates from the Fractional Black–Scholes European Option Pricing Equation (FBSEOPE) that substitutes temporal derivatives with a Caputo fractional derivative of order β. An error analysis is performed to confirm the effectiveness of the suggested method. The paper illustrates graphical representations of solution behaviors for the FBSEOPEs at various β values. A comparative study indicates that the newly developed algorithm attains higher accuracy and precision than the baseline scheme; a quantitative assessment of computational cost and runtime is left for future work. The simulation findings validate the efficacy of the suggested approach in attaining synchronization objectives and indicate its potential to be applied to other fractional models. The calculations were performed using Mathematica 13.2 and MATLAB R2020a.

Keywords. Fractional Black–Scholes European option pricing model, Fractional novel analytical scheme, Fractional novel analytic genetic algorithm, Genetic algorithm.

2010 Mathematics Subject Classification. 91G20, 26A33, 65K10, 35R11.

Uncorrected

1. Introduction

The Black–Scholes (B-S) model is a fundamental concept in contemporary finance. It offers a mathematical structure for evaluating the prospective worth of derivatives that are linked to financial instruments, taking into account elements such as time and different types of risk. The Black–Scholes model, initially developed in 1973, has become a fundamental tool for pricing options contracts [8].Merton's subsequent advancements further extended the range of applications for the Classical Black–Scholes Equation (CBSE). This equation calculates the theoretical value of an option contract by considering variables such as current stock prices, strike prices, expected dividends, expiration time, interest rates, and volatility.

Over the years, various enhancements to the B-S model have been suggested, such as transaction cost models [4, 40], jump diffusion models [5, 31, 36], stochastic volatility models [27], and stochastic interest rate models [10]. The identification of fractal patterns in financial markets led to the replacement of the conventional Brownian motion used in the CBSE with fractional Brownian motion, resulting in the development of the Fractional Black–Scholes (FBS) model [9]. Significant applications of this approach encompass the FBS pricing model for arbitrage and replication [38], pricing models for financial options in fractal transmission systems [26], the tempered Fractional Black–Scholes Equation (FBSE) for European double barrier options [41], FBS models with stochastic volatility [18], and diverse implementations in pricing double barrier options [13], options under constant elasticity of variance models [32, 35], FBS model with European option [33], and two-dimensional FBSEs [30].

Received: 19 December 2025; Accepted: 10 November 2026.
∗ Corresponding author. Email: mariamsultana@uok.edu.pk.

The motivation for adopting the fractional formulation stems from well-documented limitations of the classical model. Empirical asset-price series display memory and hereditary effects, long-range dependence, and heavy-tailed, non-Gaussian fluctuations that the classical Markovian Brownian framework cannot reproduce. Replacing the integer-order time derivative with a Caputo fractional derivative of order β allows the model to retain the influence of the entire price history through its nonlocal kernel, providing a more realistic description of option-price dynamics and improving agreement with observed volatility behaviour.

A time-space FBS European option pricing model [14] arising in the financial market is given as

$$D_t^{\beta}\ V(S,t) + \frac{1}{2}\sigma^2\ S^2\ D_S^2\ V(S,t) + (r-D)\ S\ D_S V(S,t) - r\ V(S,t) = 0, \tag{1.1}$$

here $(S,t) \in (0,S)\times(0,t)$, here β and γ are parameters describing the order of the time and space-fractional derivatives in the Caputo fractional operator sense, respectively. In (1.1) $V(S,t)$ is the European option price at asset or stock price S and at time t , t is the maturity time, $\sigma(S,t)$ is the volatility of the return function of underlying asset, $r(t)$ is the risk-free interest rate and $D(t)$ is the dividend rate. Let us denote by $C(S,t)$ and $P(S,t)$ the values of the European call and put options, respectively. Then, the payoff functions are

$$C(S,t) = \max(S-K,0)P(S,t) = \max(K-S,0), \tag{1.2}$$

where K is the expiration price or the option (the truncation bound K is chosen based on the asset price range, e.g., $K = 100$ in numerical experiments, to ensure all relevant option payoffs are captured) and the function $\max(x,0)$ gives the larger value between x and 0. With the wide application of FBSEs in option pricing, an increasing interest has been attracted on the exploration of solution techniques.

The increasing use of Fractional Black–Scholes Equations (FBSEs) for option pricing has sparked a desire to develop solution methods. Since the early 2000s, a multitude of studies have focused on seeking solutions from both analytical and numerical viewpoints. The pure integral transform technique, which is an analytical approach, provides explicit answers in the form of convolutions that involve specific functions such as the Fox function and the Mittag-Leffler function [39]. In spite of these endeavors, obtaining explicit analytical answers for FBSEs continues to be difficult in the majority of instances. Therefore, numerous techniques have been suggested to acquire (approximate) analytical solutions in the shape of infinite series. These methods include the Laplace homotopy perturbation method [24], the Laplace Legendre wavelet method [16], the Laplace homotopy analysis method [25], the residual power series method [15], the Adomian decomposition method [37], the differential transform method [11], and the Elzaki transform method [17]. From a quantitative standpoint, different finite difference approaches are frequently used. Recently, novel finite difference coupling strategies have emerged for the numerical approximation of the FBS model. These techniques involve the integration of finite difference with other methods like as the meshless method [14, 28], collocation method [33], and spectral method [19]. In addition, several more efficient numerical techniques have been developed, such as the moving least-squares method [13], space-time spectral method [6], operational matrix method [23], and neural network techniques [42].

Although there have been significant attempts to analyses FBSEs and create effective solution methods, as far as we know, the combination of metaheuristic techniques with new analytical approaches has not been documented before. This paper focuses on the fractional Black–Scholes European option pricing model with a Caputo fractional derivative in time. The general time–space fractional formulation given in (1.1) is included as a framework drawn from the literature, whereas the proposed FNAGA method is developed and applied to the time-fractional case in which the spatial derivatives remain of integer order. The model is optimized using a novel metaheuristic optimization technique. These strategies are formulated by combining traditional and modern mathematical analytical concepts. The fractional Black–Scholes European option pricing model is improved by efficiently implementing classical schemes, which are accelerated by a robust metaheuristic optimization method that mimics human evolutionary behavior. The main characteristics of the presented algorithms are their high level of precision and fast convergence. This is done by optimizing the fitness function, which is generated using the Genetic Algorithm (GA) in a mean square sense.

The paper is organized in the following manner: Section 2 presents a concise summary of fundamental definitions of Caputo fractional operator. Section 3 provides a comprehensive overview of the basic structure of the evolutionary algorithm employed to solve the fractional Black–Scholes European option pricing problems. Section 4 provides the

Uncorrected Proof

numerical solutions for the equations used to price European options in the fractional Black–Scholes model. Section 5 contains an analysis of the results, while Section 6 serves as the last section of the study.

2. Preliminaries

This section provides fundamental definitions of the Caputo fractional calculus theory.

Definition 2.1. [29] The Fractional Integral (FI) I_t^β of $V(S,t)$ is defined as:

$$I_t^\beta V(S,t) = \frac{1}{\Gamma\beta}\int_0^t (t-\xi)^{\beta-1}\, V(S,\xi)d\xi,\ \ \xi>0,\ \ m-1<\beta\le m,\ \ m\in N. \tag{2.1}$$

Definition 2.2. [29] The Caputo fractional derivative of $V(S,t)$ is defined as:

$$D_t^\beta V(S,t) = \begin{cases} \dfrac{1}{\Gamma(m-\beta)}\int_0^t (t-\xi)^{m-\beta-1}\ \dfrac{\partial^m V(S,\xi)}{\partial\xi^m}d\xi = I_t^{m-\beta}D_t^m V(S,t), & m-1<\beta<m, \\ \dfrac{\partial^m V(S,t)}{\partial t^m}, & \beta=m, \end{cases} \tag{2.2}$$

here $\dfrac{\partial^m V(S,t)}{\partial t^m}$ denotes the m^{th}-order partial derivatives, see [29] for further details.

Definition 2.3. [29] A product rule can be defined as:

$$D_t^\beta\left[V(S,t)F(S,t)\right] = \sum_{m=0}^{\infty}\binom{\beta}{m}\left[D_t^{\beta-m}V(S,t)\right]\left[D_t^\beta F(S,t)\right], \tag{2.3}$$

when $m>\beta$, the term $D_t^{\beta-m}$ is called a fractional integral and is denoted by $I_t^{m-\beta}$.

3. Basic concept of newly proposed algorithm

In order to investigate the numerical outcome of fractional Black–Scholes European option pricing equation, the Fractional Novel Analytic Scheme (FNAS) [7] along with the optimization procedures based on the Genetic Algorithm (GA) is employed. We named this new technique as Fractional Novel Analytic Genetic Algorithm (FNAGA). The Caputo fractional derivative is taken into consideration. We will discuss the idea of constructing a proposed new algorithm for the given models in this section. Consider the fractional Black–Scholes European option pricing equation in general form:

$$D_t^\beta\ V(S,t) = -\frac{1}{2}\sigma^2\ S^2\ D_S^2\ V(S,t) - (r-D)\ S\ D_S V(S,t) + r\ V(S,t),\quad t\in[t_0,t]\ \ S\in[S_0,S]\ \ 0<\beta\le 1, \tag{3.1}$$

written as

$$D_t^\beta\ V(S,t) = B\left(S,t,\sigma,r,D,V(S,t),\ D_S V(S,t),\ D_S^2\ V(S,t)\right), \tag{3.2}$$

with initial condition

$$V(S,t_0) = \max(S-K,0). \tag{3.3}$$

Now taking FI I_t^β on both sides of (3.2), we get

$$\check{V}(S,t) = \max(S-K,0) + I_t^\beta\mathcal{V}\left[V(S,t)\right], \tag{3.4}$$

where $\mathcal{V}\left[V(S,t)\right] = B\left(S,t,\sigma,r,D,V(S,t),\ D_S V(S,t),\ D_S^2\ V(S,t)\right)$. The fractional Taylor series expansions is extended for $\mathcal{V}\left[V(S,t)\right]$, which is

$$\mathcal{V}\left[V(S,t)\right] = \sum_{k=0}^{\infty}\frac{D_t^{k\beta}\mathcal{V}\left[V(S,t_0)\right]}{\Gamma(k\beta+1)}\left(t-t_0\right)^{k\beta},\qquad \beta>0. \tag{3.5}$$

Uncorrected Proof

Substituting (3.5) into (3.4), we get

$$\begin{aligned}\check{V}(S,t) &= \max(S-K,0) + \frac{\mathcal{V}\left[V\left(S,t_0\right)\right]t^{\beta}}{\Gamma(\beta+1)} + \frac{D_t^{\beta}\mathcal{V}\left[V\left(S,t_0\right)\right]t^{2\beta}}{\Gamma(2\beta+1)} + \frac{D_t^{2\beta}\mathcal{V}\left[V\left(S,t_0\right)\right]t^{3\beta}}{\Gamma(3\beta+1)} + \cdots \\ &+ \frac{D_t^{(k-1)\beta}\mathcal{V}\left[V\left(S,t_0\right)\right]t^{k\beta}}{\Gamma(k\beta+1)} + \frac{D_t^{k\beta}\mathcal{V}\left[V\left(S,t_0\right)\right]t^{(k+1)\beta}}{\Gamma\left((k+1)\beta+1\right)} + \cdots .\end{aligned} \tag{3.6}$$

$$\check{V}(S,t) = C_0 + \frac{C_1 t^{\beta}}{\Gamma(\beta+1)} + \frac{C_2 t^{2\beta}}{\Gamma(2\beta+1)} + \frac{C_3 t^{3\beta}}{\Gamma(3\beta+1)} + \cdots + \frac{C_k t^{k\beta}}{\Gamma(k\beta+1)} + \cdots . \tag{3.7}$$

We write (3.7) as

$$\check{V}(S,t) = \sum_{k=0}^{\infty} \frac{C_k t^{k\beta}}{\Gamma(k\beta+1)}, \tag{3.8}$$

here $C_0, C_1, C_2, \cdots$ are coefficients which are to be determined and M represents the number of coefficients i.e., $C_0, C_1, C_2, \cdots, C_M$. Now constructing a fitness function (F_F) given as

$$\begin{aligned}F_F = \min \sum_{j=1}^{N}\sum_{l=1}^{N} \Bigg(\check{V}(S_j,t_l) - \Bigg(\Big| D_t^{\beta}\,\widetilde{V}(S_j,t_l) - B\big(S_j,t_l,\sigma,r,D,\widetilde{V}(S_j,t_l), D_S\,\widetilde{V}(S_j,t_l), D_S^2\,\widetilde{V}(S_j,t_l)\big)\Big| \\ + \Big| V_0 - \big(\widetilde{V}\big)_0 \Big| \Bigg)\Bigg)^2 .\end{aligned} \tag{3.9}$$

In a genetic algorithm, N represents the total number of variables that are present in the domain that is being considered, $\check{V}$ is an initial approximation by FNAS and $\widetilde{V}$ is required solution by new algorithm.

The algorithm commences by creating an initial population of potential solutions to the problem. Every individual in this group is symbolized by a chromosome that encodes genetic information. The population size and chromosomal structure are customized to suit the particular challenge at hand. The fitness of each individual is assessed using a personalized fitness function, F_F, which quantifies their proficiency in solving the task. Parents for reproduction are chosen based on their high level of fitness, using several selection procedures including fitness proportionate selection. This study employed roulette wheel selection, a method in which the likelihood of choosing an individual is directly related to its fitness level, which is depicted as sectors on a circular wheel. Once the parents are chosen, the genetic material is merged by crossover to generate new children. This study employed an intermediate crossover technique, wherein genetic material from parents is combined using a weighted average approach. Mutation is a process that brings about variation and preserves genetic variety. In this case, Gaussian mutation was used, which involved inserting random values from a Gaussian distribution to certain sections of the chromosome. The present population is maintained at a steady size by replacing the least fit people with new children. The algorithm continues to execute these steps until it achieves an ideal solution or reaches a preset number of iterations, resembling the process of evolution.

Genetic algorithms mimic the process of biological evolution by repeatedly refining a group of viable solutions. This is done by selecting and merging the most successful people to create offspring, and introducing random changes to effectively explore the range of possible solutions. This approach emulates the process of human evolution, hence augmenting the algorithm's capacity to discover optimal solutions. Figure 1 depicts the structure of proposed new algorithm.

4. Numerical applications

In this section, the numerical solution of the fractional Black–Scholes European option pricing equations endowed with Caputo fractional derivative are presented using the FNAGA. The correctness of the designed FNAGA is observed by using the comparison procedure of the obtained outcomes and the FNAS solutions. Stability analysis of

Uncorrected Proof

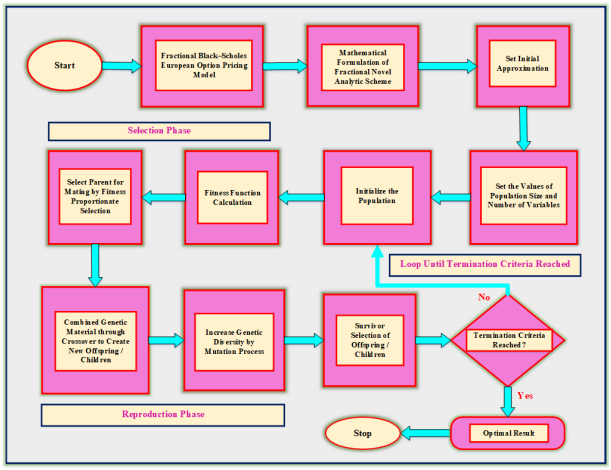


FIGURE 1. Flowchart of proposed new Fractional Novel Analytic Genetic Algorithm (FNAGA) for fractional Black–Scholes European option pricing model.

the proposed scheme follows the framework established for improved backward Euler methods for stochastic delay differential equations of neutral type [34].

Example 4.1. Consider the fractional Black–Scholes European option pricing equation [24] as:

$$D_t^{\beta}\ V(S,t) = D_S^2\ V(S,t) + (\kappa - 1)\ D_S\ V(S,t) - \kappa\ V(S,t),\ 0 < \beta \leq 1, \tag{4.1}$$

with initial condition

$$V(S,0) = \max\left(e^S - 1, 0\right). \tag{4.2}$$

Note that (4.1) contains two dimensionless parameters $\kappa = \frac{2r}{\sigma^2}$, where κ represents the balance between the rate of interests and the variability of stock returns and the dimensionless time to expiry $\frac{\sigma^2 t}{2}$, even though there are four dimensional parameters, σ^2, t, K, r in the original statements of the problem. The exact solution is given as $V(S,t) = \max\left(e^S - 1, 0\right) e^{-\kappa\ t} + \max\left(e^S, 0\right)\left(1 - e^{-\kappa\ t}\right)$ at $\beta = 1$. After carefully following the procedures outlined in section 3, calculating six coefficients i.e., $C_0, C_1, C_2, C_3, C_4, C_5$. Substitute these coefficient values in (3.8) and set the initial approximation $\check{V}(S,t)$. The fitness formulation of (4.1) is given as

$$\begin{aligned} F_F = \min \sum_{j=1}^{N} \sum_{l=1}^{N} \Bigg(\check{V}(S_j,t_l) - \Bigg(\Big| D_t^{\beta}\ \widetilde{V}(S_j,t_l) - D_S^2\ \widetilde{V}(S_j,t_l) - (\kappa - 1)\ D_S\ \widetilde{V}(S_j,t_l) + \kappa\ \widetilde{V}(S_j,t_l) \Big| \\ + \Big| \max(e^{S_j} - 1, 0) - \left(\widetilde{V}\right)_0 \Big| \Bigg) \Bigg)^2. \end{aligned} \tag{4.3}$$

Example 4.2. Consider the generalized fractional Black–Scholes European option pricing equations [24] as:

$$D_t^{\beta}\ V(S,t) = -0.08 S^2\ (2 + \sin S)^2\ D_S^2\ V(S,t) - 0.06\ S D_S V(S,t) + 0.06\ V(S,t),\ 0 < \beta \leq 1, \tag{4.4}$$

with initial condition

$$V(S,0) = \max\left(S - 25\ e^{-0.06}, 0\right). \tag{4.5}$$

The exact solution is given as $V(S,t) = \max\left(S - 25\ e^{-0.06}, 0\right) e^{-0.06\ t} + S\left(1 - e^{-0.06\ t}\right)$ at $\beta = 1$. After carefully following the procedures outlined in Section 3, calculating six coefficients i.e., $C_0, C_1, C_2, C_3, C_4, C_5$. Substitute these

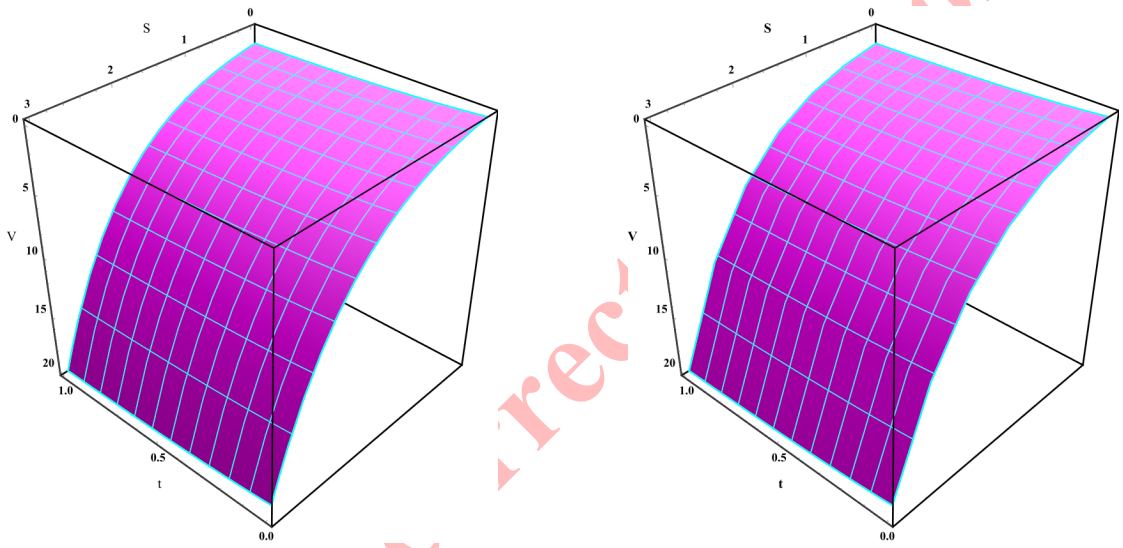
Uncorrected Proof

coefficient values in (3.8) and set the initial approximation $\check{V}(S,t)$. The fitness formulation of (4.4) is given as

$$F_F = \min \sum_{j=1}^{N}\sum_{l=1}^{N}\left(\check{V}(S_j,t_l) - \left(\left|D_t^{\beta}\widetilde{V}(S_j,t_l) + 0.08{S_j}^2(2+\sin^2 S_j)D_S^2\widetilde{V}(S_j,t_l) + 0.06S_j D_S\widetilde{V}(S_j,t_l)\right.\right.\right.$$
$$\left.\left.\left. - 0.06\widetilde{V}(S_j,t_l)\right| + \left|\max(S_j - 25\,e^{-0.06},0) - \left(\widetilde{V}\right)_0\right|\right)\right)^2. \tag{4.6}$$

5. Result Analysis

The optimization approach for fractional Black–Scholes European option pricing equations and running FNAGA for 1000 generations with a population size of 8000 to obtain FNAGA solutions for $N = 40$. In this approach, the roulette wheel selection method is used for parent selection based on fitness proportionality during mating, with a crossover probability (P_c) of 0.8. An intermediate crossover function is used during reproduction to produce offspring. In addition, genetic diversity among the offspring is increased by applying a mutation process with a Gaussian mutation technique, which includes a mutation probability (P_m) of 0.01.



(A) Exact solution. (B) FNAGA solution.

Figure 2. At $\beta = 1$, $\kappa = 2$ and $N = 40$, the result of the obtained solution by using FNAGA and exact solution to solve the Example 4.1 are presented.

Figure 2(A) and 2(B) graphically display the exact and FNAGA obtained solution for the Example 4.1 at $\beta = 1$, $\kappa = 2$, $S \in [0,3]$, $t \in [0,1]$ and $N = 40$ numbers of variables. The results generated via FNAGA closely resemble the exact solution, indicating that the suggested approach is accurate and correct. Figure 3 displays the solution of Example 4.1 by FNAGA with various values of β (i.e., $\beta = 0.5, 0.6, 0.7, 0.8, 0.9$) with $N = 40$, $\kappa = 2$ and $S, t \in [0,1]$. At various β values, the solution derived via FNAGA demonstrates its behaviour.

F_σ's (fitness values) and K_M (Mean Square Error) values obtained from FNAGA to solve the Example 4.1 at different values of $S \in [0,3]$ and $N = 40, 50, 60, 100$ are shown graphically in Figures 4(A) and 4(B) with $\beta = 1$, $\kappa = 2$ and $t \in [0,1]$. In Figure 5(A), with $\kappa = 2$, $N = 40$, and $t \in [0,1]$, the F_σ's derived by FNAGA to solve the Example 4.1 for various values of S and β are graphically displayed. The graphical view of K_A (Absolute Error) values derived by FNAGA for the Example 4.1 with $N = 40$ number of variables at $\beta = 1$, $\kappa = 2$, $S \in [0,2]$, $t \in [0,1]$ is illustrated in Figure 5(B). The FNAGA is used to solve Example 4.1, and the outcomes are accomplished satisfactorily.

Uncorrected Proof

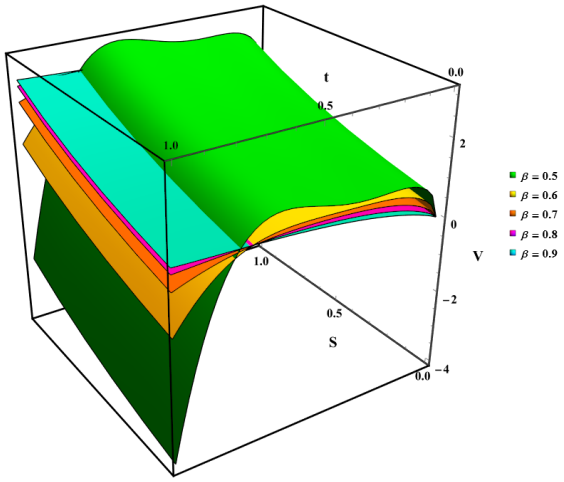
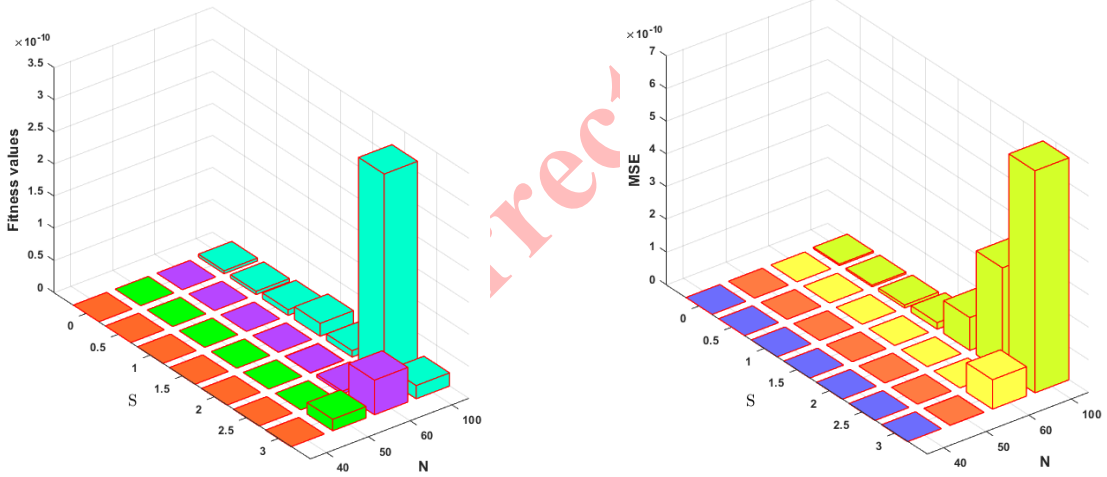


FIGURE 3. Visual representations of the solution found by FNAGA for the Example 4.1 at various values of β with $\kappa = 2$, $N = 40$.

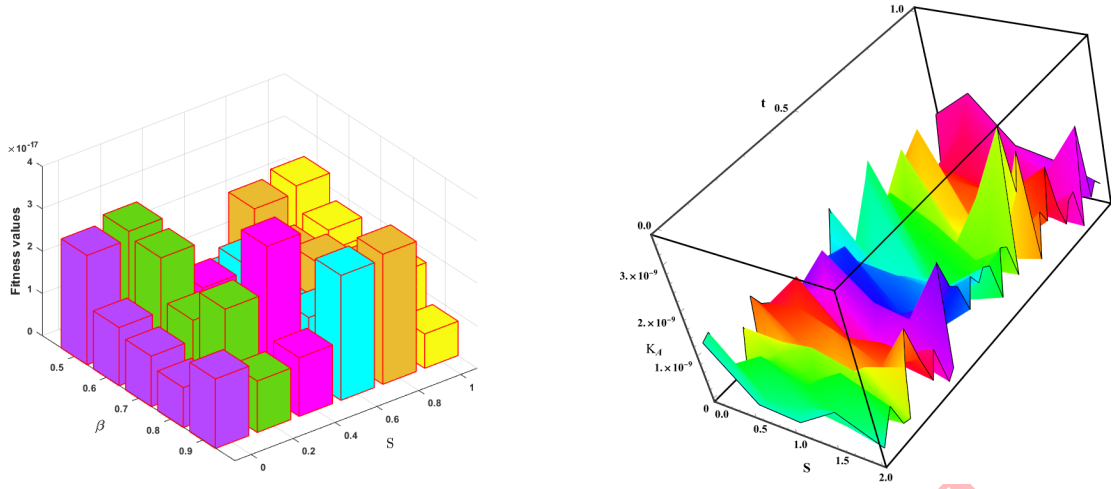
Proof



(A) F_σ's. (B) K_M.

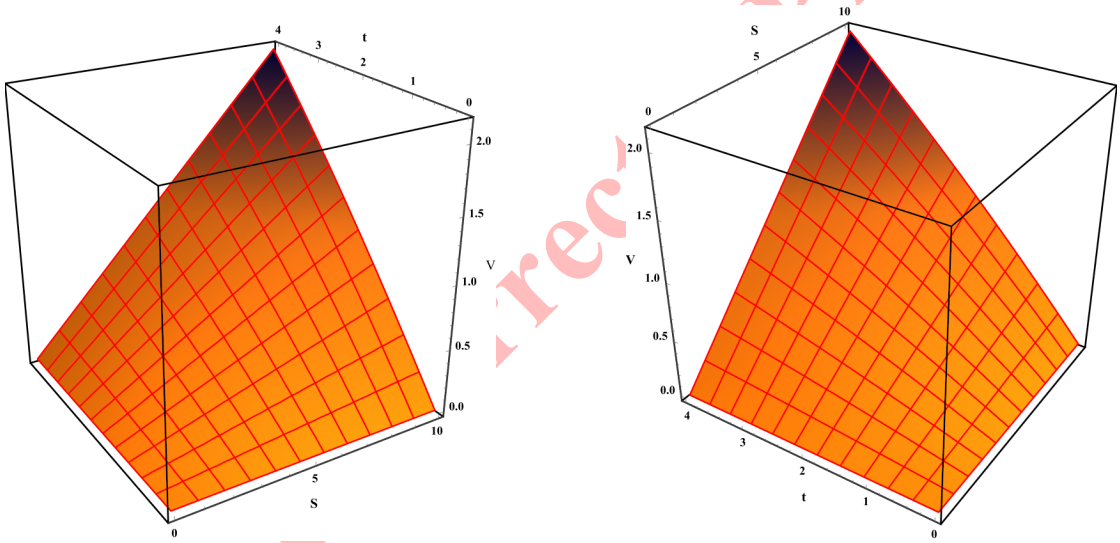
FIGURE 4. Bar graphs of (A) F_σ's and (B) K_M values obtained by FNAGA at $\beta = 1$, $\kappa = 2$, $t \in [0, 1]$ with different values of N to solve the Example 4.1.

Table 1 display the K_M and F_σ's attained from FNAGA and FNAS to solve the Example 4.1 at $\beta = 1$, $\kappa = 2$ with varying numbers of variables N, $S \in [0, 3]$ and $t \in [0, 1]$. When compare to FNAS, the K_M values derived using FNAGA are significantly lower. These K_M values provide evidence that FNAGA is accurate in resolving the Example 4.1. Table 2 compares the FNAGA numerical finding with the exact solution to the Example 4.1 at $\beta = 1$, $\kappa = 2$, and $N = 40$ for various values of $S = 1, 2, 3$. The accuracy of the proposed new algorithm is clearly illustrated, as FNAGA produces that are identical to the exact solution. Table 3 compares the K_A values to the Example 4.1 generating



(A) F_σ's at different values of β. (B) K_A.

FIGURE 5. (A) Bar graphs of F_σ's and (B) graphical representation of K_A values obtained by FNAGA to solve Example 4.1 with $\kappa = 2$, $N = 40$ and $t \in [0, 1]$.



(A) Exact solution. (B) FNAGA solution.

FIGURE 6. At $\beta = 1$ and $N = 40$, the results of the obtained solution by using FNAGA and exact solution to solve the Example 4.2 are presented.

by FNAGA and FNAS with $N = 40$ variables. According to the FNAGA results, the performance in resolving the Example 4.1 is adequate. For broader methodological context, the accuracy achieved here can be viewed alongside other modern solution strategies for Black–Scholes-type models and fractional differential equations, including the multiple shooting method [2], efficient algorithms for pricing European, barrier, and American options [1], operational matrix and B-spline wavelet constructions [3, 12], flatlet oblique multiwavelet Galerkin approaches [21], fractional second linear multistep methods [20], and generating functions built on linear barycentric rational interpolation [22]. A direct numerical comparison with all of these schemes lies beyond the scope of the present study, in which FNAS

serves as the primary baseline; a systematic benchmarking of FNAGA against such methods on common test problems is planned as future work.

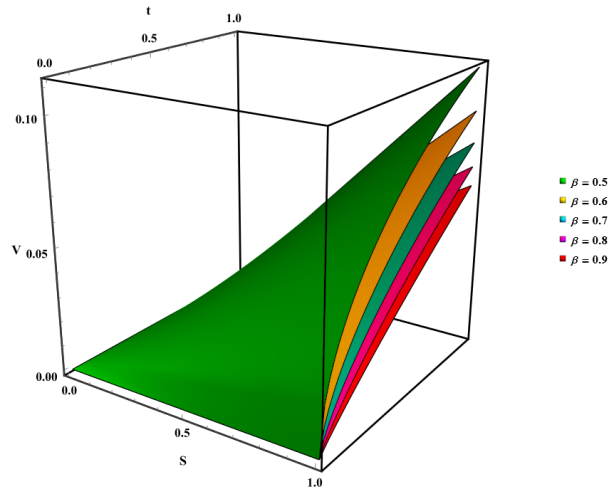
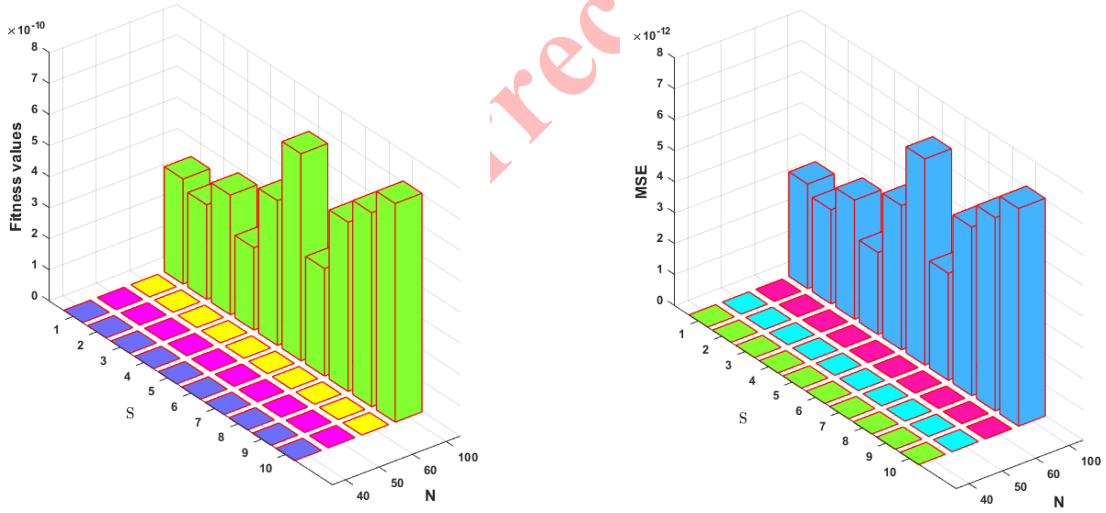


FIGURE 7. Visual representations of the solution found by FNAGA for the Example 4.2 with $N = 40$ at various values of β.

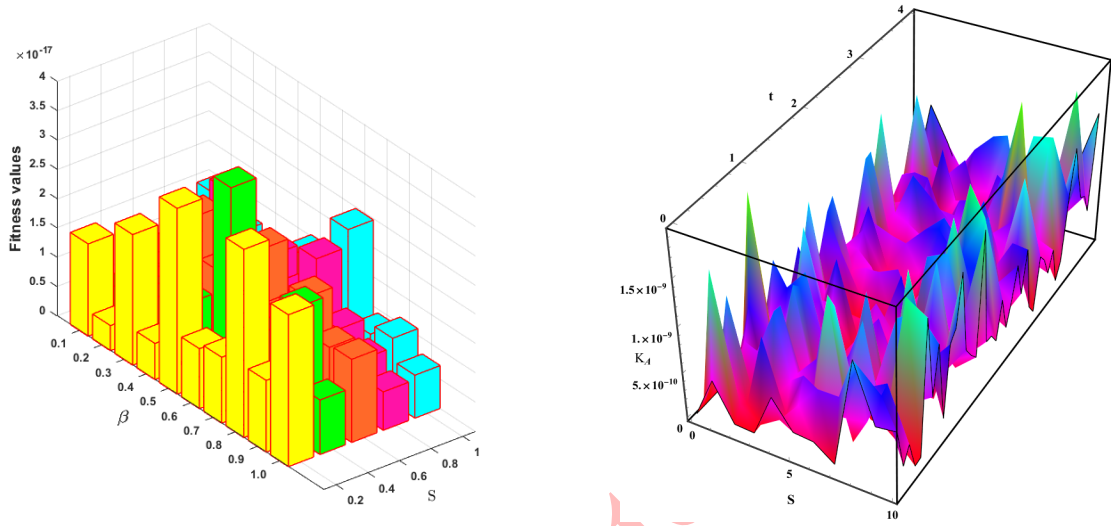


(A) F_σ's. (B) K_M.

FIGURE 8. Bar graphs of (A) F_σ's and (B) K_M values obtained by FNAGA to solve the Example 4.2 with different values of N at $\beta = 1$, $\kappa = 2$, and $t \in [0, 4]$.

The exact and FNAGA solutions for Example 4.2 at $\beta = 1$, $S \in [0, 10]$, $t \in [0, 4]$, and $N = 40$ number of variables is shown graphically in Figures 6(A) and 6(B). A comparable output from FNAGA and the exact solution serves to

illustrate that the algorithm is valid and accurate. The solutions of Example 4.2 by FNAGA with different values of β i.e., $\beta = 0.5, 0.6, 0.7, 0.8, 0.9$ at $N = 40$, $S, t \in [0, 1]$ is shown in Figure 7. The solution obtained by FNAGA exhibits its behavior at different β values. In Figures 8(A) and 8(B) displays bar graphs for several values of $S \in [0, 10]$ and $N = 40, 50, 60, 100$. The K_M and F_σ's were derived by solving Example 4.2 at $\beta = 1$ and $t \in [0, 4]$ using FNAGA. Figure 9(A), with $N = 40$, $t \in [0, 1]$, displays the F_σ's produced via FNAGA to solve the Example 4.2 at various values of $S = 0.2, 0.4, 0.6, 0.8, 1.0$, and $\beta \in [0, 1]$. Figure 9(B) shows the graphical view of K_A values for the Example 4.2 that were derived by FNAGA with $N = 40$ at $\beta = 1$, $S \in [0, 10]$, and $t \in [0, 4]$. Using the FNAGA to solve Example 4.2, the results are completed satisfactorily.



(A) F_σ's at different values of β. (B) K_A.

FIGURE 9. (A) Bar graphs of F_σ's and (B) graphical representation of K_A values obtained by FNAGA to solve Example 4.2 with $N = 40$.

In order to solve Example 4.2 at $\beta = 1$ with varying number of variables N, S and $t \in [0, 4]$, Table 4 displays the K_M values of FNAS, FNAGA and F_σ's derived via FNAGA. When compared to FNAS, the K_M values derived using FNAGA are significantly lower. Finding support the accuracy of FNAGA in resolving the Example 4.2 based on these K_M values. Table 5 presents a comparison between the Example 4.2 at $\beta = 1$, $t \in [0, 4]$ with $N = 40$ for various values of S and the numerical results from the FNAGA with the precise solution. FNAGA produces results that are nearly identical to the exact solution, which established the correctness of the proposed new algorithm. Considering $t \in [0, 4]$ at $\beta = 1$ for various values of S, Table 6 compares the K_A values to the Example 4.2 produced by FNAGA and FNAS with $N = 40$ variables. Example 4.2 can be solved with satisfactory performance, according to the FNAGA results.

6. Conclusion

This work utilizes a unique technique and optimization procedure employing the evolutionary algorithm to conduct numerical studies for solving fractional Black–Scholes European option pricing equations. The fractional derivative is evaluated using the Caputo meaning. The subsequent findings are as follows:

- The results derived from the numerical solution of the FBSEs were graphically and tabularly compared to the exact solution. The results obtained from the FNAGA are comparable to the exact solution, demonstrating that the proposed algorithm is accurate.
- The K_A values have been provided with 40 variables for the purpose of solving the FBSE. This error analysis was done to validate the precision, competency, and validity of the FNAGA methods.

Uncorrected

TABLE 1. The K_M and F_σ's attained from FNAGA and FNAS to solve the Example 4.1 at $\beta = 1$, $\kappa = 2$ and $t \in [0, 1]$ with different values of N and S.

S	N	Mean square error (K_M) values		FNAGA fitness values (F_σ's)
		FNAS	FNAGA	
0.0	40	4.2783×10^{-4}	4.0429×10^{-19}	1.6171×10^{-17}
	50	4.1686×10^{-4}	1.7674×10^{-17}	8.8371×10^{-16}
	60	4.0968×10^{-4}	5.4962×10^{-16}	3.2977×10^{-14}
	100	3.9565×10^{-4}	4.6132×10^{-12}	4.6132×10^{-12}
0.5	40	4.2783×10^{-4}	1.2482×10^{-18}	4.9928×10^{-17}
	50	4.1686×10^{-4}	1.6113×10^{-17}	8.0565×10^{-16}
	60	4.0968×10^{-4}	3.9624×10^{-16}	2.3775×10^{-14}
	100	3.9565×10^{-4}	5.0712×10^{-12}	5.0712×10^{-12}
1.0	40	4.2783×10^{-4}	2.8140×10^{-19}	1.1256×10^{-17}
	50	4.1686×10^{-4}	3.7845×10^{-17}	1.8923×10^{-15}
	60	4.0968×10^{-4}	8.5512×10^{-16}	5.1307×10^{-14}
	100	3.9565×10^{-4}	8.9863×10^{-12}	8.9863×10^{-12}
1.5	40	4.2783×10^{-4}	3.8991×10^{-19}	1.5596×10^{-17}
	50	4.1686×10^{-4}	2.7238×10^{-17}	1.3619×10^{-15}
	60	4.0968×10^{-4}	2.3476×10^{-15}	1.4085×10^{-13}
	100	3.9565×10^{-4}	2.0016×10^{-11}	2.0016×10^{-11}
2.0	40	4.2783×10^{-4}	1.7621×10^{-18}	7.0486×10^{-17}
	50	4.1686×10^{-4}	1.1559×10^{-16}	5.7796×10^{-15}
	60	4.0968×10^{-4}	8.3029×10^{-15}	4.9817×10^{-13}
	100	3.9565×10^{-4}	1.0033×10^{-10}	1.0033×10^{-11}
2.5	40	4.2783×10^{-4}	5.7947×10^{-18}	2.3179×10^{-16}
	50	4.1686×10^{-4}	1.1759×10^{-15}	5.8796×10^{-14}
	60	4.0968×10^{-4}	7.1936×10^{-14}	4.3162×10^{-12}
	100	3.9565×10^{-4}	3.1726×10^{-10}	3.1726×10^{-10}
3.0	40	4.2783×10^{-4}	6.7789×10^{-16}	2.7116×10^{-14}
	50	4.1686×10^{-4}	3.5814×10^{-13}	1.7907×10^{-11}
	60	4.0968×10^{-4}	8.9789×10^{-11}	5.3874×10^{-11}
	100	3.9565×10^{-4}	6.7884×10^{-10}	2.0546×10^{-11}

- To solve the FBSE, the reliability is acquired by observing the K_M values. When applied to various FBSEs, the approach provided produces exceptional results. The fact that it is a one-time run method, which means that it does not need to be repeated multiple times, is one of the most appealing aspects of this algorithm.
- Compared to other approach (FNAS), the numerical example demonstrates how accurate and efficient the strategy presented in this work is.

In the future, we will also utilize this method for various circumstances, such as fractional biological equations and other models. Additionally, extending the proposed hybrid FNAGA method to three-asset options or to Black–Scholes models with time-dependent coefficients would further demonstrate the flexibility and broad applicability of the approach.

Uncorrected Proof

ACKNOWLEDGMENT

This work forms part of the Ph.D. thesis of the first author, carried out under the supervision of the corresponding author. The authors thank the anonymous reviewers for their valuable comments and suggestions, which improved the quality of the manuscript.

TABLE 2. Comparing the numerical results from the FNAGA with the exact solution to the Example 4.1 at $\beta = 1$, $\kappa = 2$ and $N = 40$ for different values of $S = 1, 2, 3$.

t	$V_{\text{Exact}}(1,t)$	$V_{\text{FNAGA}}(1,t)$	$V_{\text{Exact}}(2,t)$	$V_{\text{FNAGA}}(2,t)$	$V_{\text{Exact}}(3,t)$	$V_{\text{FNAGA}}(3,t)$
0.000000	1.718282	1.718282	6.389056	6.389056	19.085537	19.085537
0.025641	1.768271	1.768271	6.439045	6.439045	19.135526	19.135526
0.051282	1.815762	1.815762	6.486536	6.486536	19.183017	19.183017
0.076923	1.860878	1.860878	6.531652	6.531652	19.228133	19.228133
0.102564	1.903739	1.903739	6.574513	6.574513	19.270994	19.270994
0.128205	1.944457	1.944457	6.615232	6.615232	19.311712	19.311712
0.153846	1.983140	1.983140	6.653915	6.653915	19.350395	19.350395
0.179487	2.019890	2.019890	6.690664	6.690664	19.387145	19.387145
0.205128	2.054802	2.054802	6.725576	6.725576	19.422057	19.422057
0.230769	2.087969	2.087969	6.758743	6.758743	19.455224	19.455224
0.256410	2.119478	2.119478	6.790252	6.790252	19.486733	19.486733
0.282051	2.149411	2.149411	6.820186	6.820186	19.516666	19.516666
0.307692	2.177849	2.177849	6.848623	6.848623	19.545104	19.545104
0.333333	2.204865	2.204865	6.875639	6.875639	19.572120	19.572120
0.358974	2.230530	2.230530	6.901304	6.901304	19.597785	19.597785
0.384615	2.254912	2.254912	6.925687	6.925687	19.622168	19.622168
0.410256	2.278076	2.278076	6.948850	6.948850	19.645331	19.645331
0.435897	2.300082	2.300082	6.970856	6.970856	19.667337	19.667337
0.461538	2.320987	2.320987	6.991761	6.991761	19.688242	19.688242
0.487179	2.340848	2.340848	7.011622	7.011622	19.708103	19.708103
0.512821	2.359715	2.359715	7.030490	7.030490	19.726970	19.726970
0.538462	2.377640	2.377640	7.048414	7.048414	19.744895	19.744895
0.564103	2.394668	2.394668	7.065443	7.065443	19.761923	19.761923
0.589744	2.410845	2.410845	7.081620	7.081620	19.778101	19.778101
0.615385	2.426214	2.426214	7.096988	7.096988	19.793469	19.793469
0.641026	2.440814	2.440814	7.111589	7.111589	19.808069	19.808069
0.666667	2.454685	2.454685	7.125459	7.125459	19.821940	19.821940
0.692308	2.467862	2.467862	7.138636	7.138636	19.835117	19.835117
0.717949	2.480380	2.480380	7.151154	7.151154	19.847635	19.847635
0.743590	2.492273	2.492273	7.163047	7.163047	19.859528	19.859528
0.769231	2.503571	2.503571	7.174345	7.174345	19.870826	19.870826
0.794872	2.514304	2.514304	7.185078	7.185078	19.881559	19.881559
0.820513	2.524501	2.524501	7.195275	7.195275	19.891756	19.891756
0.846154	2.534188	2.534188	7.204962	7.204962	19.901443	19.901443
0.871795	2.543390	2.543390	7.214165	7.214165	19.910645	19.910645
0.897436	2.552133	2.552133	7.222907	7.222907	19.919388	19.919388
0.923077	2.560439	2.560439	7.231213	7.231213	19.927694	19.927694
0.948718	2.568329	2.568329	7.239103	7.239103	19.935584	19.935584
0.974359	2.575825	2.575825	7.246600	7.246600	19.943080	19.943080
1.000000	2.582947	2.582947	7.253721	7.253721	19.950202	19.950202

Uncorrected Proof

TABLE 3. Comparison of K_A values obtained from FNAGA and FNAS to solve the Example 4.1 at $\beta = 1$, $\kappa = 2$ and $N = 40$ for different values of $S = 1, 2, 3$.

t	$K_A^{\mathrm{FNAS}}(1,t)$	$K_A^{\mathrm{FNAGA}}(1,t)$	$K_A^{\mathrm{FNAS}}(2,t)$	$K_A^{\mathrm{FNAGA}}(2,t)$	$K_A^{\mathrm{FNAS}}(3,t)$	$K_A^{\mathrm{FNAGA}}(3,t)$
0.000000	0.00000	3.5870×10^{-11}	0.00000	1.9400×10^{-10}	0.00000	2.6516×10^{-9}
0.025641	2.5080×10^{-11}	2.5410×10^{-10}	2.5079×10^{-11}	5.0465×10^{-10}	2.5100×10^{-11}	2.5350×10^{-8}
0.051282	1.5933×10^{-9}	5.5026×10^{-10}	1.5934×10^{-9}	7.9468×10^{-10}	1.5933×10^{-9}	1.1349×10^{-8}
0.076923	1.8019×10^{-8}	5.2664×10^{-10}	1.8019×10^{-8}	2.4113×10^{-10}	1.8019×10^{-8}	2.8165×10^{-8}
0.102564	1.0052×10^{-7}	1.1096×10^{-9}	1.0052×10^{-7}	1.8349×10^{-10}	1.0052×10^{-7}	3.6310×10^{-8}
0.128205	3.8070×10^{-7}	2.1321×10^{-10}	3.8070×10^{-7}	1.1612×10^{-9}	3.8070×10^{-7}	1.3634×10^{-8}
0.153846	1.1287×10^{-6}	5.3630×10^{-11}	1.1287×10^{-6}	1.8441×10^{-9}	1.1287×10^{-6}	3.4616×10^{-8}
0.179487	2.8262×10^{-6}	1.0581×10^{-9}	2.8262×10^{-6}	1.0227×10^{-9}	2.8262×10^{-6}	5.3966×10^{-8}
0.205128	6.2531×10^{-6}	7.4008×10^{-10}	6.2531×10^{-6}	3.8731×10^{-10}	6.2531×10^{-6}	2.5482×10^{-8}
0.230769	1.2588×10^{-5}	4.4716×10^{-10}	1.2588×10^{-5}	9.3991×10^{-10}	1.2588×10^{-5}	3.2653×10^{-8}
0.256410	2.3523×10^{-5}	1.5642×10^{-10}	2.3523×10^{-5}	3.9330×10^{-11}	2.3523×10^{-5}	8.8066×10^{-9}
0.282051	4.1385×10^{-5}	7.7730×10^{-11}	4.1385×10^{-5}	1.9964×10^{-10}	4.1385×10^{-5}	3.6999×10^{-8}
0.307692	6.9277×10^{-5}	2.3010×10^{-11}	6.9277×10^{-5}	2.3520×10^{-9}	6.9277×10^{-5}	7.8507×10^{-9}
0.333333	1.1122×10^{-4}	7.6800×10^{-10}	1.1122×10^{-4}	1.6995×10^{-9}	1.1122×10^{-4}	2.8617×10^{-8}
0.358974	1.7232×10^{-4}	2.1327×10^{-10}	1.7232×10^{-4}	1.5544×10^{-9}	1.7232×10^{-4}	2.6418×10^{-8}
0.384615	2.5892×10^{-4}	1.6578×10^{-10}	2.5892×10^{-4}	8.9930×10^{-10}	2.5892×10^{-4}	3.7151×10^{-8}
0.410256	3.7881×10^{-4}	1.5929×10^{-10}	3.7881×10^{-4}	1.4837×10^{-9}	3.7881×10^{-4}	1.1191×10^{-8}
0.435897	5.4135×10^{-4}	8.1084×10^{-10}	5.4135×10^{-4}	1.1975×10^{-9}	5.4135×10^{-4}	2.9211×10^{-8}
0.461538	7.5775×10^{-4}	6.6254×10^{-10}	7.5775×10^{-4}	1.3941×10^{-9}	7.5775×10^{-4}	6.9866×10^{-9}
0.487179	1.0412×10^{-3}	3.1205×10^{-10}	1.0412×10^{-3}	1.2910×10^{-9}	1.0412×10^{-3}	9.6455×10^{-9}
0.512821	1.4071×10^{-3}	4.2000×10^{-10}	1.4071×10^{-3}	4.3497×10^{-10}	1.4071×10^{-3}	3.0247×10^{-8}
0.538462	1.8733×10^{-3}	5.5500×10^{-11}	1.8733×10^{-3}	1.4029×10^{-9}	1.8733×10^{-3}	4.4059×10^{-9}
0.564103	2.4603×10^{-3}	8.3697×10^{-12}	2.4603×10^{-3}	1.2874×10^{-9}	2.4603×10^{-3}	6.6080×10^{-10}
0.589744	3.1915×10^{-3}	5.3644×10^{-10}	3.1915×10^{-3}	5.2212×10^{-10}	3.1915×10^{-3}	6.5501×10^{-9}
0.615385	4.0935×10^{-3}	1.0207×10^{-9}	4.0935×10^{-3}	3.5582×10^{-9}	4.0935×10^{-3}	1.6993×10^{-8}
0.641026	5.1960×10^{-3}	1.1827×10^{-10}	5.1960×10^{-3}	2.0741×10^{-9}	5.1960×10^{-3}	4.0745×10^{-8}
0.666667	6.5327×10^{-3}	1.8857×10^{-10}	6.5327×10^{-3}	2.8186×10^{-9}	6.5327×10^{-3}	4.1768×10^{-8}
0.692308	8.1408×10^{-3}	2.9789×10^{-10}	8.1408×10^{-3}	3.2043×10^{-10}	8.1408×10^{-3}	2.9252×10^{-8}
0.717949	1.0062×10^{-2}	2.9392×10^{-10}	1.0062×10^{-2}	1.2550×10^{-9}	1.0062×10^{-2}	1.1392×10^{-8}
0.743590	1.2342×10^{-2}	5.6595×10^{-10}	1.2342×10^{-2}	9.1963×10^{-10}	1.2342×10^{-2}	3.6072×10^{-8}
0.769231	1.5031×10^{-2}	1.4755×10^{-10}	1.5031×10^{-2}	1.9901×10^{-9}	1.5031×10^{-2}	2.8259×10^{-8}
0.794872	1.8186×10^{-2}	1.8799×10^{-10}	1.8186×10^{-2}	9.9963×10^{-10}	1.8186×10^{-2}	1.5417×10^{-8}
0.820513	2.1866×10^{-2}	8.0494×10^{-10}	2.1866×10^{-2}	4.4466×10^{-10}	2.1866×10^{-2}	1.4791×10^{-8}
0.846154	2.6138×10^{-2}	5.6372×10^{-10}	2.6138×10^{-2}	8.5746×10^{-10}	2.6138×10^{-2}	5.4996×10^{-8}
0.871795	3.1074×10^{-2}	4.6847×10^{-10}	3.1074×10^{-2}	9.3390×10^{-10}	3.1074×10^{-2}	1.5038×10^{-9}
0.897436	3.6751×10^{-2}	3.8069×10^{-10}	3.6751×10^{-2}	5.5067×10^{-13}	3.6751×10^{-2}	8.2913×10^{-9}
0.923077	4.3255×10^{-2}	2.7727×10^{-10}	4.3255×10^{-2}	2.1412×10^{-9}	4.3255×10^{-2}	1.2052×10^{-8}
0.948718	5.0676×10^{-2}	5.9187×10^{-10}	5.0676×10^{-2}	4.1551×10^{-10}	5.0676×10^{-2}	4.3629×10^{-9}
0.974359	5.9112×10^{-2}	8.8128×10^{-10}	5.9112×10^{-2}	6.6463×10^{-10}	5.9112×10^{-2}	2.1434×10^{-8}
1.000000	6.8669×10^{-2}	9.5140×10^{-10}	6.8669×10^{-2}	4.7728×10^{-10}	6.8669×10^{-2}	2.7494×10^{-8}

Uncorrected Proof

TABLE 4. K_M values of FNAGA, FNAS and F_σ's obtained via FNAGA to solve the Example 4.2 at $\beta = 1$, $t \in [0, 4]$ with different values of N, S.

S	N	Mean square error (K_M) values		FNAGA fitness values (F_σ's)
		FNAS	FNAGA	
1.0	40	5.826347×10^{-15}	6.469331×10^{-19}	2.587733×10^{-17}
	50	5.671983×10^{-15}	2.823646×10^{-17}	1.411823×10^{-15}
	60	5.570999×10^{-15}	3.625813×10^{-16}	2.175488×10^{-14}
	100	5.373596×10^{-15}	3.382482×10^{-12}	3.382482×10^{-10}
2.0	40	2.330539×10^{-14}	2.321605×10^{-19}	9.286422×10^{-18}
	50	2.268793×10^{-14}	2.335116×10^{-17}	1.167558×10^{-15}
	60	2.228400×10^{-14}	3.430951×10^{-16}	2.058571×10^{-14}
	100	2.149438×10^{-14}	3.044156×10^{-12}	3.044156×10^{-10}
3.0	40	5.243712×10^{-14}	3.538151×10^{-19}	1.415261×10^{-17}
	50	5.104784×10^{-14}	1.600352×10^{-17}	8.001759×10^{-16}
	60	5.013900×10^{-14}	3.389985×10^{-16}	2.033991×10^{-14}
	100	4.836236×10^{-14}	3.850219×10^{-12}	3.850219×10^{-10}
4.0	40	9.322154×10^{-14}	1.634445×10^{-19}	6.537778×10^{-18}
	50	9.075172×10^{-14}	1.142143×10^{-17}	5.710714×10^{-16}
	60	8.913599×10^{-14}	3.839786×10^{-16}	2.303872×10^{-14}
	100	8.597753×10^{-14}	2.650081×10^{-12}	2.650081×10^{-10}
5.0	40	1.456587×10^{-13}	1.828868×10^{-19}	7.315453×10^{-18}
	50	1.417996×10^{-13}	5.964831×10^{-17}	2.982416×10^{-15}
	60	1.392750×10^{-13}	3.367335×10^{-16}	2.020401×10^{-14}
	100	1.343399×10^{-13}	4.662834×10^{-12}	4.662834×10^{-10}
6.0	40	2.097485×10^{-13}	3.906528×10^{-19}	1.562611×10^{-17}
	50	2.041914×10^{-13}	2.407422×10^{-17}	1.203711×10^{-15}
	60	2.005560×10^{-13}	4.464708×10^{-16}	2.678825×10^{-14}
	100	1.934494×10^{-13}	6.665061×10^{-12}	6.665061×10^{-10}
7.0	40	2.854910×10^{-13}	2.997026×10^{-19}	1.198812×10^{-17}
	50	2.779271×10^{-13}	1.435137×10^{-17}	7.175689×10^{-16}
	60	2.729790×10^{-13}	6.335173×10^{-16}	3.801104×10^{-14}
	100	2.633062×10^{-13}	3.460897×10^{-12}	3.460897×10^{-10}
8.0	40	3.728862×10^{-13}	7.680700×10^{-19}	3.072276×10^{-17}
	50	3.630069×10^{-13}	3.146329×10^{-17}	1.573165×10^{-15}
	60	3.565440×10^{-13}	5.442863×10^{-16}	3.265718×10^{-14}
	100	3.439101×10^{-13}	5.449647×10^{-12}	5.449647×10^{-10}
9.0	40	4.719341×10^{-13}	6.481880×10^{-19}	2.592757×10^{-17}
	50	4.594306×10^{-13}	8.514969×10^{-17}	4.257485×10^{-15}
	60	4.512510×10^{-13}	9.027639×10^{-16}	5.416584×10^{-14}
	100	4.352612×10^{-13}	6.249604×10^{-12}	6.249604×10^{-10}
10.0	40	5.826347×10^{-13}	5.513643×10^{-19}	2.205460×10^{-17}
	50	5.671983×10^{-13}	1.321348×10^{-17}	6.606738×10^{-16}
	60	5.570999×10^{-13}	6.572267×10^{-16}	3.943360×10^{-14}
	100	5.373596×10^{-13}	7.039145×10^{-12}	7.039145×10^{-10}

Uncorrected Proof

TABLE 5. With $N = 40$ and different values of S, comparing of the numerical results from the FNAGA with the precise solution to solve the Example 4.2 at $\beta = 1$.

t	$V_{\text{Exact}}(1,t)$	$V_{\text{FNAGA}}(1,t)$	$V_{\text{Exact}}(5,t)$	$V_{\text{FNAGA}}(5,t)$	$V_{\text{Exact}}(10,t)$	$V_{\text{FNAGA}}(10,t)$
0.000000	0.000000	0.000000	0.000000	0.000000	0.000000	0.000000
0.102564	0.006135	0.006135	0.030675	0.030675	0.061350	0.061350
0.205128	0.012232	0.012232	0.061161	0.061161	0.122323	0.122323
0.307692	0.018292	0.018292	0.091461	0.091461	0.182922	0.182922
0.410256	0.024315	0.024315	0.121574	0.121574	0.243149	0.243149
0.512821	0.030301	0.030301	0.151503	0.151503	0.303007	0.303007
0.615385	0.036250	0.036250	0.181249	0.181249	0.362497	0.362497
0.717949	0.042162	0.042162	0.210811	0.210811	0.421623	0.421623
0.820513	0.048039	0.048039	0.240193	0.240193	0.480386	0.480386
0.923077	0.053879	0.053879	0.269394	0.269394	0.538788	0.538788
1.025641	0.059683	0.059683	0.298416	0.298416	0.596832	0.596832
1.128205	0.065452	0.065452	0.327260	0.327260	0.654520	0.654520
1.230769	0.071185	0.071185	0.355927	0.355927	0.711854	0.711854
1.333333	0.076884	0.076884	0.384418	0.384418	0.768837	0.768837
1.435897	0.082547	0.082547	0.412735	0.412735	0.825469	0.825469
1.538462	0.088175	0.088175	0.440877	0.440877	0.881755	0.881755
1.641026	0.093769	0.093769	0.468847	0.468847	0.937695	0.937695
1.743590	0.099329	0.099329	0.496646	0.496646	0.993291	0.993291
1.846154	0.104855	0.104855	0.524274	0.524274	1.048547	1.048547
1.948718	0.110346	0.110346	0.551732	0.551732	1.103464	1.103464
2.051282	0.115804	0.115804	0.579022	0.579022	1.158044	1.158044
2.153846	0.121229	0.121229	0.606144	0.606144	1.212289	1.212289
2.256410	0.126620	0.126620	0.633100	0.633100	1.266201	1.266201
2.358974	0.131978	0.131978	0.659891	0.659891	1.319782	1.319782
2.461538	0.137303	0.137303	0.686517	0.686517	1.373035	1.373035
2.564103	0.142596	0.142596	0.712980	0.712980	1.425961	1.425961
2.666667	0.147856	0.147856	0.739281	0.739281	1.478562	1.478562
2.769231	0.153084	0.153084	0.765420	0.765420	1.530841	1.530841
2.871795	0.158280	0.158280	0.791399	0.791399	1.582799	1.582799
2.974359	0.163444	0.163444	0.817219	0.817219	1.634438	1.634438
3.076923	0.168576	0.168576	0.842880	0.842880	1.685760	1.685760
3.179487	0.173677	0.173677	0.868384	0.868384	1.736767	1.736767
3.282051	0.178746	0.178746	0.893731	0.893731	1.787462	1.787462
3.384615	0.183785	0.183785	0.918923	0.918923	1.837845	1.837845
3.487179	0.188792	0.188792	0.943960	0.943960	1.887920	1.887920
3.589744	0.193769	0.193769	0.968844	0.968844	1.937687	1.937687
3.692308	0.198715	0.198715	0.993574	0.993574	1.987149	1.987149
3.794872	0.203631	0.203631	1.018154	1.018154	2.036307	2.036307
3.897436	0.208516	0.208516	1.042582	1.042582	2.085164	2.085164
4.000000	0.213372	0.213372	1.066861	1.066861	2.133721	2.133721

Uncorrected Proof

TABLE 6. Comparison of K_A values obtained from FNAGA and FNAS to solve the Example 4.2 at $\beta = 1$ and $N = 40$ for different values of $S = 1, 5, 10$.

t	$K_A^{\mathrm{FNAS}}(1,t)$	$K_A^{\mathrm{FNAGA}}(1,t)$	$K_A^{\mathrm{FNAS}}(5,t)$	$K_A^{\mathrm{FNAGA}}(5,t)$	$K_A^{\mathrm{FNAS}}(10,t)$	$K_A^{\mathrm{FNAGA}}(10,t)$
0.000000	0.000000	4.550×10^{-10}	0.00000	2.203×10^{-10}	0.00000	6.646×10^{-10}
0.102564	1.102×10^{-16}	1.562×10^{-9}	6.002×10^{-16}	4.422×10^{-10}	1.103×10^{-15}	2.072×10^{-10}
0.205128	4.800×10^{-15}	4.045×10^{-10}	2.400×10^{-14}	6.861×10^{-10}	4.800×10^{-14}	3.618×10^{-10}
0.307692	5.490×10^{-14}	1.156×10^{-9}	2.744×10^{-13}	2.688×10^{-10}	5.490×10^{-13}	3.405×10^{-11}
0.410256	3.078×10^{-13}	1.764×10^{-10}	1.540×10^{-12}	7.142×10^{-10}	3.078×10^{-12}	4.621×10^{-11}
0.512821	1.174×10^{-12}	5.114×10^{-10}	5.867×10^{-12}	1.854×10^{-10}	1.174×10^{-11}	1.457×10^{-9}
0.615385	3.501×10^{-12}	8.315×10^{-10}	1.750×10^{-11}	2.872×10^{-10}	3.501×10^{-11}	5.522×10^{-10}
0.717949	8.820×10^{-12}	1.948×10^{-9}	4.410×10^{-11}	1.276×10^{-11}	8.820×10^{-11}	1.043×10^{-9}
0.820513	1.964×10^{-11}	2.512×10^{-10}	9.818×10^{-11}	2.821×10^{-10}	1.964×10^{-10}	1.527×10^{-10}
0.923077	3.977×10^{-11}	4.747×10^{-10}	1.989×10^{-10}	4.144×10^{-12}	3.977×10^{-10}	8.927×10^{-10}
1.025641	7.477×10^{-11}	1.052×10^{-9}	3.739×10^{-10}	3.550×10^{-10}	7.477×10^{-10}	9.871×10^{-10}
1.128205	1.323×10^{-10}	2.449×10^{-11}	6.617×10^{-10}	4.343×10^{-10}	1.323×10^{-9}	1.500×10^{-9}
1.230769	2.229×10^{-10}	6.613×10^{-11}	1.114×10^{-9}	2.435×10^{-10}	2.229×10^{-9}	6.017×10^{-10}
1.333333	3.600×10^{-10}	1.461×10^{-10}	1.800×10^{-9}	3.441×10^{-10}	3.600×10^{-9}	4.704×10^{-10}
1.435897	5.610×10^{-10}	9.332×10^{-10}	2.805×10^{-9}	5.882×10^{-10}	5.610×10^{-9}	3.708×10^{-10}
1.538462	8.480×10^{-10}	6.874×10^{-10}	4.240×10^{-9}	3.010×10^{-10}	8.480×10^{-9}	1.660×10^{-9}
1.641026	1.248×10^{-9}	1.290×10^{-9}	6.240×10^{-9}	5.749×10^{-11}	1.248×10^{-8}	3.963×10^{-10}
1.743590	1.794×10^{-9}	1.942×10^{-10}	8.969×10^{-9}	1.137×10^{-10}	1.794×10^{-8}	3.883×10^{-10}
1.846154	2.526×10^{-9}	7.145×10^{-10}	1.263×10^{-8}	6.937×10^{-10}	2.526×10^{-8}	2.577×10^{-10}
1.948718	3.490×10^{-9}	9.936×10^{-10}	1.745×10^{-8}	1.489×10^{-10}	3.490×10^{-8}	6.458×10^{-10}
2.051282	4.744×10^{-9}	1.107×10^{-9}	2.372×10^{-8}	5.561×10^{-11}	4.744×10^{-8}	2.643×10^{-10}
2.153846	6.352×10^{-9}	1.988×10^{-10}	3.176×10^{-8}	6.250×10^{-11}	6.352×10^{-8}	5.080×10^{-10}
2.256410	8.390×10^{-9}	4.263×10^{-10}	4.195×10^{-8}	3.866×10^{-10}	8.390×10^{-8}	8.225×10^{-10}
2.358974	1.094×10^{-8}	2.270×10^{-10}	5.472×10^{-8}	8.073×10^{-10}	1.094×10^{-7}	4.359×10^{-10}
2.461538	1.412×10^{-8}	3.488×10^{-10}	7.058×10^{-8}	6.048×10^{-10}	1.412×10^{-7}	8.659×10^{-10}
2.564103	1.802×10^{-8}	6.094×10^{-10}	9.009×10^{-8}	3.243×10^{-10}	1.802×10^{-7}	1.438×10^{-10}
2.666667	2.278×10^{-8}	1.155×10^{-9}	1.139×10^{-7}	1.062×10^{-10}	2.278×10^{-7}	1.861×10^{-11}
2.769231	2.854×10^{-8}	1.179×10^{-9}	1.427×10^{-7}	1.720×10^{-10}	2.854×10^{-7}	5.846×10^{-10}
2.871795	3.547×10^{-8}	2.366×10^{-10}	1.774×10^{-7}	5.769×10^{-10}	3.547×10^{-7}	4.783×10^{-10}
2.974359	4.375×10^{-8}	1.485×10^{-9}	2.187×10^{-7}	5.877×10^{-10}	4.375×10^{-7}	2.619×10^{-10}
3.076923	5.357×10^{-8}	1.830×10^{-11}	2.679×10^{-7}	7.018×10^{-10}	5.357×10^{-7}	4.622×10^{-10}
3.179487	6.516×10^{-8}	3.467×10^{-10}	3.258×10^{-7}	2.576×10^{-10}	6.516×10^{-7}	3.569×10^{-11}
3.282051	7.877×10^{-8}	2.399×10^{-10}	3.938×10^{-7}	5.033×10^{-11}	7.877×10^{-7}	2.061×10^{-10}
3.384615	9.466×10^{-8}	5.597×10^{-10}	4.733×10^{-7}	5.155×10^{-10}	9.466×10^{-7}	8.699×10^{-10}
3.487179	1.131×10^{-7}	5.224×10^{-10}	5.657×10^{-7}	1.354×10^{-10}	1.131×10^{-6}	1.357×10^{-9}
3.589744	1.345×10^{-7}	4.377×10^{-10}	6.725×10^{-7}	1.322×10^{-10}	1.345×10^{-6}	9.907×10^{-10}
3.692308	1.591×10^{-7}	1.311×10^{-9}	7.957×10^{-7}	4.401×10^{-10}	1.591×10^{-6}	6.847×10^{-10}
3.794872	1.874×10^{-7}	3.794×10^{-10}	9.371×10^{-7}	1.018×10^{-9}	1.874×10^{-6}	6.399×10^{-10}
3.897436	2.197×10^{-7}	3.426×10^{-10}	1.099×10^{-6}	5.305×10^{-10}	2.197×10^{-6}	4.086×10^{-10}
4.000000	2.566×10^{-7}	1.036×10^{-9}	1.283×10^{-6}	3.750×10^{-11}	2.566×10^{-6}	1.457×10^{-9}

Uncorrected Proof

References

[1] S. Abdi-Mazraeh, and A. Khani, *An efficient computational algorithm for pricing European, barrier and American options*, Computational and Applied Mathematics, *37* (2018), 4856–4876.

[2] S. Abdi-Mazraeh, A. Khani, and S. Irandoust-Pakchin, *Multiple shooting method for solving Black–Scholes equation*, Computational Economics, *56*(4) (2020), 723–746.

[3] S. Abdi-Mazraeh, H. Kheiri, and S. Irandoust-Pakchin, *Construction of operational matrices based on linear cardinal B-spline functions for solving fractional stochastic integro-differential equation*, Journal of Applied Mathematics and Computing, *68* (2022), 151–175.

[4] J. I. Adindu-Dick, *Optimal trading using Black-Scholes equation with transaction costs*, African Journal of Mathematics and Statistics Studies, *5*(2) (2022), 1–9.

[5] D. Ahmadian, L. V. Ballestra, and N. Karimi, *An extremely efficient numerical method for pricing options in the Black–Scholes model with jumps*, Mathematical Methods in the Applied Sciences, *44* (2021), 1843–1862.

[6] X. An, F. Liu, M. Zheng, V. V. Anh, and I. W. Turner, *A space-time spectral method for time-fractional Black–Scholes equation*, Applied Numerical Mathematics, *165* (2021), 152–166.

[7] U. Arshad, and M. Sultana, *On the numerical evaluation for studying the time fractional partial delay differential equations*, Punjab University Journal of Mathematics, *56*(12) (2024), 799–820.

[8] F. Black, and M. Scholes, *The pricing of options and corporate liabilities*, Journal of Political Economy, *81*(3) (1973), 637–654.

[9] J. Blackledge, and M. Lamphiere, *A review of the fractal market hypothesis for trading and market price prediction*, Mathematics, *10*(1) (2022), 117.

[10] C. Cai, T. De Angelis, and J. Palczewski, *The American put with finite-time maturity and stochastic interest rate*, Mathematical Finance, Wiley Blackwell, *32*(4) (2022), 1170–1213.

[11] S. O. Edeki, R. M. Jena, S. Chakraverty, and D. Baleanu, *Coupled transform method for time-space fractional Black–Scholes option pricing model*, Alexandria Engineering Journal, *59*(5) (2020), 3239–3246.

[12] A. Elahi, S. Irandoust-Pakchin, A. Rahimi, and S. Abdi-Mazraeh, *A new approach of B-spline wavelets to solve fractional differential equations*, Communications in Nonlinear Science and Numerical Simulation, *136* (2024), 108099.

[13] A. Golbabai, and O. Nikan, *A computational method based on the moving least-squares approach for pricing double barrier options in a time-fractional Black-Scholes model*, Computational Economic, *55* (2020), 119–141.

[14] A. Golbabai, O. Nikan, and T. Nikazad, *Numerical analysis of time fractional Black-Scholes European option pricing model arising in financial market*, Computational and Applied Mathematics, *38*(173) (2019).

[15] S. Haq and M. Hussain, *Selection of shape parameter in radial basis functions for solution of time fractional Black-Scholes models*, Applied Mathematics and Computation, *335*(C) (2018), 248–263.

[16] G. Hariharan, S. Padma, and P. Pirabaharan, *An efficient wavelet based approximation method to time fractional Black-Scholes European option pricing problem arising in financial market*, Applied Mathematical Sciences, *7*(69) (2013), 3445–3456.

[17] W. He, N. Chen, I. Dassios, N. A. Shah, and J. D. Chung, *Fractional system of Korteweg-de Vries equations via Elzaki transform*, Mathematics, *9*(6) (2021), 673.

[18] X. J. He, and S. Lin, *A fractional Black-Scholes model with stochastic volatility and European option pricing*, Expert Systems with Applications, *178* (2021), 114983.

[19] J. He, and A. Zhang, *Finite difference/Fourier spectral for a time fractional Black-Scholes model with option pricing*, Mathematical Problems in Engineering, (2020), 1393456, 9 pages.

[20] S. Irandoust-Pakchin, and S. Abdi-Mazraeh, *Fractional second linear multistep methods: the explicit forms for solving fractional differential equations and stability analysis*, International Journal of Computer Mathematics, *100*(1) (2023), 20–46.

[21] S. Irandoust-Pakchin, S. Abdi-Mazraeh, and M. Adel, *Application of flatlet oblique multiwavelets to solve the fractional stochastic integro-differential equation using Galerkin method*, Mathematical Methods in the Applied Sciences, *47*(11) (2024), 8324–8365.

Uncorrected Proof

[22] S. Irandoust-Pakchin, S. Abdi-Mazraeh, and H. Kheiri, *Construction of new generating function based on linear barycentric rational interpolation for numerical solution of fractional differential equations*, Journal of Computational and Applied Mathematics, *375* (2020), 112799.
[23] Y. Kumar, and V. K. Singh, *Computational approach based on wavelets for financial mathematical model governed by distributed order fractional differential equation*, Mathematics and Computers in Simulation, *190*(C) (2021), 531–569.
[24] S. Kumar, A. Yildirim, Y. Khan, H. Jafari, K. Sayevand, and L. Wei, *Analytical solution of fractional Black–Scholes European option pricing equation by using Laplace transform*, Journal of Fractional Calculus and Applications, (2012).
[25] Ö. Necati, *A different approach to the European option pricing model with new fractional operator*, Mathematical Modelling of Natural Phenomena, (2018).
[26] O. Nikan, Z. Avazzadeh, and J. A. T. Machado, *Localized kernel-based meshless method for pricing financial options underlying fractal transmission system*, Mathematical Methods in the Applied Sciences, *47*(5) (2024), 3247–3260.
[27] A. H. Nzokem, *Pricing European options under stochastic volatility models: Case of five-parameter variance-gamma process*, Journal of Risk and Financial Management, *16*(1) (2023), 55.
[28] P. Phaochoo, A. Luadsong, and N. Aschariyaphotha, *The meshless local Petrov-Galerkin based on moving kriging interpolation for solving fractional Black-Scholes model*, Journal of King Saud University - Science, *28*(1) (2016), 111–117.
[29] I. Podlubny, *Fractional Differential Equations*, Academic Press, San Diego, California, 1999.
[30] D. Prathumwan, and K. Trachoo, *On the solution of two-dimensional fractional Black-Scholes equation for European put option*, Advances in Difference Equations, *2020*(146) (2020).
[31] A. Rathinasamy, D. Ahmadian, and P. Nair, *Second-order balanced stochastic Runge–Kutta methods with multi-dimensional studies*, Journal of Computational and Applied Mathematics, *377* (2020), 112890.
[32] M. Rezaei, A. R. Yazdanian, A.R. Ashrafi, and S. M. Mahmoudi, *Numerical pricing based on fractional Black–Scholes equation with time-dependent parameters under the CEV model: Double barrier options*, Computers & Mathematics with Applications, *90* (2021), 104–111.
[33] P. Roul, *A high accuracy numerical method and its convergence for time-fractional Black-Scholes equation governing European options*, Applied Numerical Mathematics, *151* (2020), 472–493.
[34] O. F. Rouz, and D. Ahmadian, *Stability of two classes of improved backward Euler methods for stochastic delay differential equations of neutral type*, Computational Methods for Differential Equations, *5*(3) (2017), 201–213.
[35] A. Safdari-Vaighani, D. Ahmadian, and R. Javid-Jahromi, *An approximation scheme for option pricing under two-state continuous CAPM*, Computational Economics, *57*(4) (2021), 1373–1385.
[36] C. Shi, *Asymptotic analysis of the mixed-exponential jump diffusion model and its financial applications*, Journal of Economic Dynamics and Control, *143* (2022), 104518.
[37] L. Song, *A semi analytical solution of the fractional derivative model and its application in financial market*, Complexity, (2018), 1872409, 10 pages.
[38] S. Tommi, and V. Esko, *On arbitrage and replication in the fractional Black-Scholes pricing model*, Statistics & Risk Modeling, De Gruyter, *21*(2) (2003), 93–108.
[39] W. Wyss, *The fractional Black-Scholes equation*, Fractional Calculus and Applied Analysis, *3* (2000), 51–61.
[40] D. Yan, *A comprehensive study of option pricing with transaction costs*, 2021, Thesis (Ph.D.)–School of Mathematics and Applied Statistics, University of Wollongong - Australia.
[41] H. M. Zhang, F. W. Liu, I. Turner, and S. Z. Chen, *The numerical simulation of the tempered fractional Black–Scholes equation for European double barrier option*, Applied Mathematical Modelling, *40* (2016), 5819–5834.
[42] X. Zhang, J. Yang, and Y. Zhao, *Numerical solution of time fractional Black-Scholes model based on Legendre wavelet neural network with extreme learning machine*, Fractal and Fractional, *6*(7) (2022), 401.

Uncorrected Proof